Available online at www.eccomasproceedia.org
Eccomas Proceedia COMPDYN (2023) 4133-4143

ECCOMAS Proceedia

COMPDYN 2023
9th ECCOMAS Thematic Conference on
Computational Methods in Structural Dynamics and Earthquake Engineering
M. Papadrakakis, M. Fragiadakis (eds.)
Athens, Greece, 12-14 June 2023

# FRAGILITY CURVES FOR A SMALL ZONED EARTH DAM

**M. Tretola**[1], **S. Sica**[1]

[1] Department of Civil Engineering, University of Sannio
Benevento, Italy
martretola@unisannio.it

**Abstract**

*The paper presents a suite of fragility curves to evaluate the seismic vulnerability of a small earth dam. The goal is to provide a user-friendly tool to estimate the expected damage of this type of barrages that, since classified as small, are typically subjected to less restricting controls than large dams with the consequent increase of their vulnerability. In this study, the incremental dynamic analysis method (IDA) was applied to a prototype of small zoned earth dam. To perform nonlinear dynamic analyses through the finite element software Plaxis2D, an advanced soil constitutive model combined to a three-phase formulation was adopted. To develop the fragility curves for each damage type relevant for the seismic performance of the dam, ten representative accelerometric signals were selected. Four damage measures (DMs) were considered, namely the settlement ratio at the dam crest, the lateral displacements of the dam crest, the freeboard reduction and the maximum plastic shear strain of the watertightness element. These damage indicators were later related to three intensity measures (IMs), i.e. PGA, PGV and the Arias Intensity. As outcome of the study, the fragility curves for different limit states of the identified DMs were obtained.*

**Keywords:** Zoned earth dam, fragility curve, damage index, intensity measure

ISSN:2623-3347 
Peer-review under responsibility of the organizing committee of COMPDYN 2023.
doi: 10.7712/120123.10707.20857

# 1 INTRODUCTION

Dam safety assessment has always been a challenging task for civil engineers due to the high risk generally associated with these structures. Actually, the direct and indirect consequences of any uncontrolled release of water from the reservoir can be catastrophic for the downstream population.

In the case of existing earth dams, the problem is further complicated by the inherent difficulty in achieving a detailed knowledge on recent and past loading history of the dam, on properties of the soil materials and their possible modification during the life of the dam.

The lack of reliable information on the original design of the structure combined to that of a thorough monitoring activity is even more critical for small earth dams, i.e. those characterized by embankments of lower height and limited reservoir capacity (H ≤ 15 m or water storage ≤ 1 million $m^3$). Despite their size, the risk associated with small dams could be comparable or even higher than that associated to larger dams. In Italy most of the existing dams (small and large) are located in areas characterized by high seismic hazard. Moreover, most of them dating back to the middle of the last century, were built without taking seismic actions into account or underestimating the seismic hazard at the dam site.

Actually, the seismic performance of these dams needs to be evaluated using more advanced analytical approaches. It is also advisable to provide the dam owners (mostly private) or the local authority in charge of the dam operation with the results of the study carried out, organized in suitable tables or charts to assess the dam safety immediately after the earthquake.

A useful tool, which is increasingly emerging in the field of earth dams as a valid alternative to the traditional deterministic methods, is represented by fragility curves. These are obtained by means of a probabilistic approach that allows the uncertainties associated with the input motion and/or soil properties to be overcome. In addition, the fragility curves represent the anticipated tool that ensures a rapid assessment of the probable damage caused by an earthquake and, in particular, the probability that a certain damage index (DI) exceeds a limit state threshold for a given intensity measure (IM) of the seismic event.

Nowadays, fragility curves have mostly been obtained for concrete and arch dams [1, 2, 3, 4]. A few studies, recently published, refer to large earth dams, mainly concrete-faced rockfill dams (CFRDs) [5, 6, 7], earth-rockfill dams [8], rockfill dams with concrete core [9, 10] and just one study (in the authors' knowledge) concerns tailing dams [11].

In this study, fragility curves were developed for a small zoned earth dam assumed to be placed in an area of medium-high seismic hazard. It represents the prototype of many small dams widespread in Italy and worldwide.

The seismic performance of the dam prototype was evaluated basing on different damage indicators computed through the incremental dynamic analysis method (IDA) using the finite element code Plaxis2D. Peak ground acceleration (PGA), peak ground velocity (PGV) and Arias intensity (AI) were selected as intensity measures (IMs). The failure likelihood for the dam prototype has been researched for the three limit states of minor, moderate, and severe damage.

# 2 MODELING OF THE CASE STUDY

The case study concerns an ideal 13m-high zoned earth dam, composed of sandy shells and a clayey core founded on a rigid foundation (Figure 1). At this stage of the work, this simple configuration of the small dam was selected to avoid site effects and foundation-soil compliance.

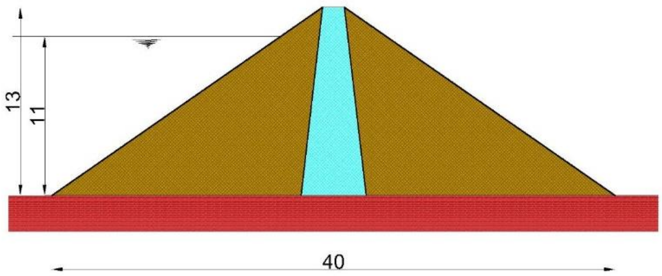


Figure 1: Geometry of the small earth dam.

The dam prototype was modeled in 2D assuming plane strain conditions. To perform the nonlinear dynamic analyses for computing the fragility curves, an elastoplastic constitutive law, defined *Hardening Soil with Small Strain Stiffness* (HS small) implemented in Plaxis2D, was assigned to the different materials of the dam body. It is an advanced constitutive law that is able to describe with sufficient accuracy the non-linear, hysteretic and plastic response of the soil from the small to the high strain levels. To account for the partial saturation of the dam soils, a three-phase formulation was adopted by assigning suitable water retention curves to the core and the shell materials through the *Van Genuchten* formulation (1980) [12]. The static analysis of the dam was preliminarily carried out by simulating the construction of the embankment and the first filling of the reservoir.

The dynamic stage was simulated considering the impounding level fixed at its maximum height ($H_w$=11 m) and by applying the input signal in the horizontal direction along the bottom boundary of the model. In addition to the hysteretic damping provided by the HS-small constitutive law, a small amount of material damping $\xi = 1\%$ (initial damping) was attributed to the dam soils through the Rayleigh formulation. The coefficients $\alpha$ and $\beta$, which are respectively proportional to the mass [M] and stiffness [K] matrix, were computed in correspondence of two target frequencies, $f_1$ and $f_2$, as proposed by Hudson et al. [13] or Hash and Park [14]. In this case, $f_1$ was set equal to 5 Hz (almost equal to the first fundamental frequency of the dam body) and $f_2=3f_1$. Table 1 summarizes the physical and mechanical parameters attributed to the dam core and shells.

| Parameters | Unit | Clayey core | Sandy shells |
|---|---|---|---|
| $\gamma_{sat}$ | *[kN/m³]* | 22 | 19.6 |
| $\gamma_{unsat}$ | *[kN/m³]* | 21 | 16.3 |
| e | *[-]* | 0.4 | 0.6 |
| $k_{sat}$ | *[m/s]* | 2.8E-10 | 3.5E-5 |
| c’ | *[kPa]* | 14 | 1 |
| φ' | *[°]* | 36 | 41 |
| ψ | *[°]* | 0 | 0 |
| $k_0$ | *[-]* | 0.4 | 0.34 |
| $E_{50}^{ref}$ | *[MPa]* | 8.5 | 19.8 |
| $E_{oed}^{ref}$ | *[MPa]* | 5.5 | 14. |
| $E_{ur}^{ref}$ | *[MPa]* | 25.5 | 59.4 |
| m | *[-]* | 0.98 | 0.5 |
| $G_0^{ref}$ | *[MPa]* | 95 | 165 |
| $\gamma_{0.7}$ | *[-]* | 1.7E-4 | 1.7E-4 |

Table 1: HS-small parameters used in the numerical analysis.

## 3 INPUT SIGNAL SELECTION

To estimate the dam vulnerability against earthquakes, it is necessary to find the relationship between the seismic motion intensity and the structural response so that the probability of exceeding a given limit state may be calculated.

| Signal ID | PGA [g] | IA [m/s] | $T_p$ [s] | $D_{5\text{-}95}$ [s] |
|---|---|---|---|---|
| #Signal_1 | 0.110 | 0.12 | 0.10 | 12.7 |
| #Signal_2 | 0.110 | 0.21 | 0.32 | 16.2 |
| #Signal_3 | 0.140 | 0.46 | 0.16 | 17.5 |
| #Signal_4 | 0.150 | 0.23 | 0.38 | 6.5 |
| #Signal_5 | 1.390 | 0.18 | 0.22 | 14.8 |
| #Signal_6 | 0.069 | 0.21 | 0.20 | 10.0 |
| #Signal_7 | 0.181 | 0.38 | 0.50 | 12.2 |
| #Signal_8 | 1.392 | 0.27 | 0.18 | 34.8 |
| #Signal_9 | 1.800 | 0.25 | 0.11 | 24.6 |
| #Signal_10 | 0.072 | 0.13 | 0.34 | 17.3 |

Table 2: Main parameters of the input signals used for the IDA.

For this purpose, a set of 10 representative acceleration time-histories were selected such that their predominant frequencies include the first natural frequency of the dam (estimated approximately around 5 Hz). Figure 2 shows the amplitude Fourier spectrum of the selected input signals. For computing the fragility curves of the dam, each natural accelerogram was scaled in magnitude from a peak acceleration of 0.11g to 0.44g, trying to avoid scale factors too high for not modifying the signal nature. Considering all waveforms in Table 2 and the 7 scale factors adopted, a total amount of 70 dynamic analyses were performed.

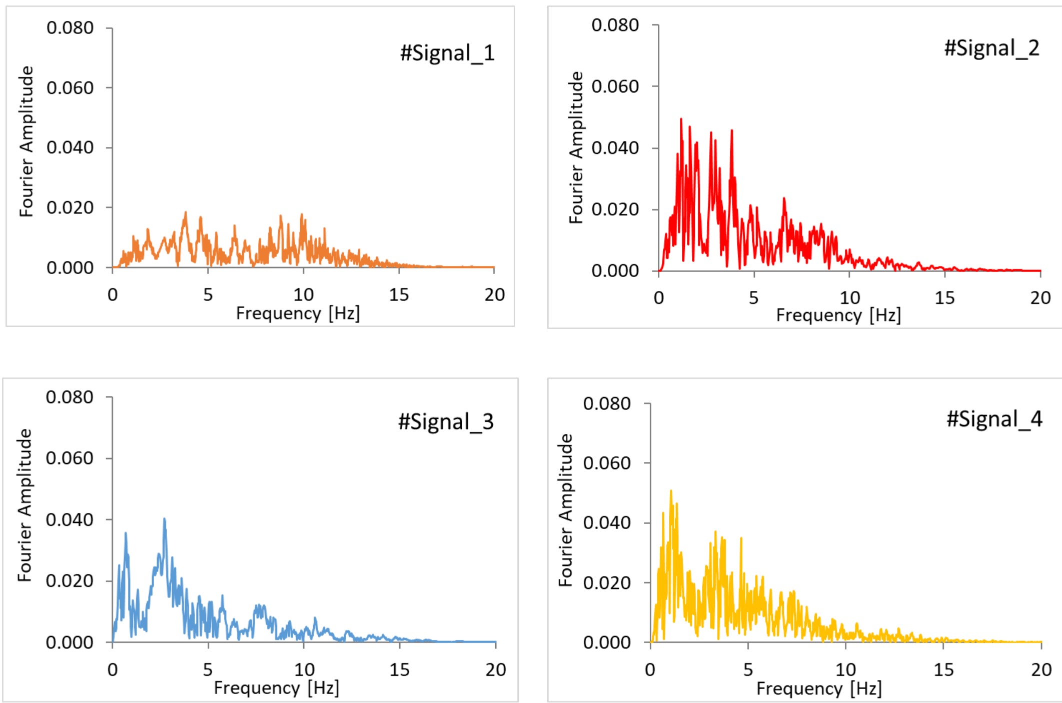

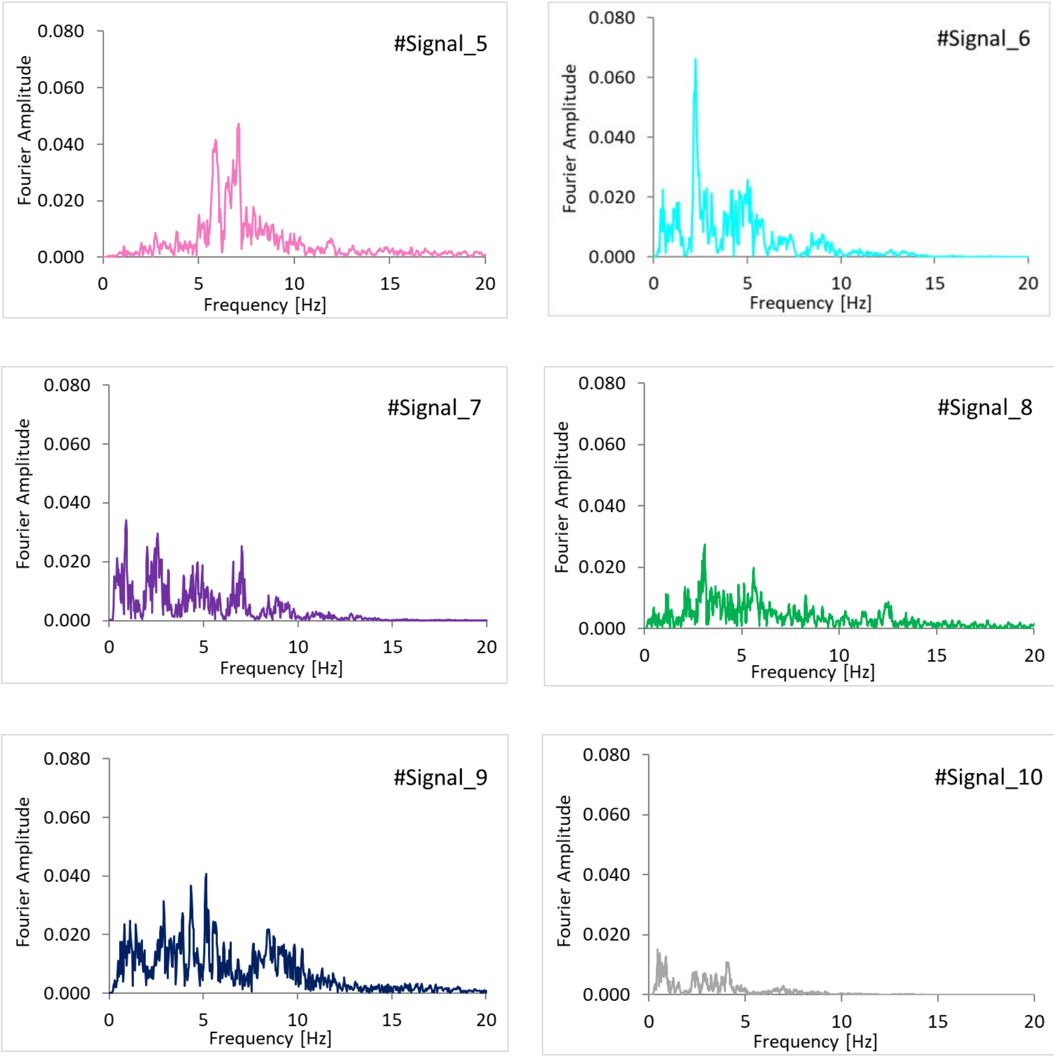


Figure 2: Fourier amplitude spectrum for all the adopted input signals.

As an example, Figure 3 shows the typical deformed configuration of the small dam at the end of the dynamic stage with the input accelerogram #Signal_1, while Figure 4 provides for the corresponding contours of vertical ($u_y$) and horizontal ($u_x$) permanent displacements. Higher displacements were computed on the upstream shell of the dam with a maximum vertical displacement of about 0.16 m and a maximum horizontal displacement of about 0.13 m. The core, instead, denotes a less deformable response.

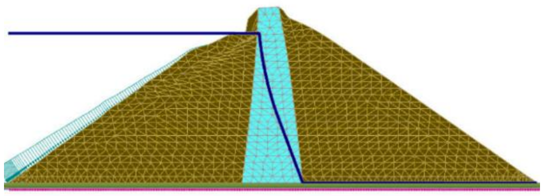

Figure 3: Deformed configuration at the end of the dynamic stage for the representative input #Signal_1.

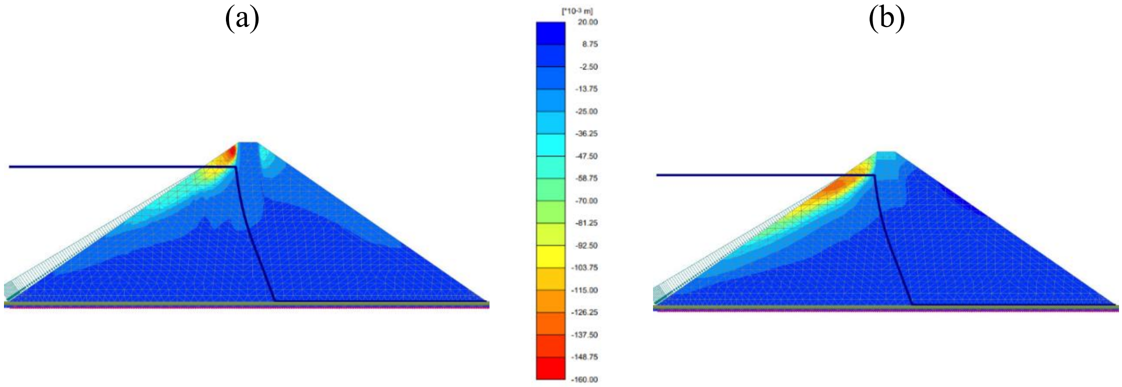


Figure 4: Contour of the (a) vertical and (b) horizontal displacements computed at the end of input #Signal_1.

# 4 FRAGILITY CURVES

## 4.1 Overview of the methodology

The fragility of a structure may be described using the statistical expression of conditional probability. Given two events A and B, it represents the probability of A occurring, knowing that B has happened:

$$P[A|B] \tag{1}$$

In the field of civil engineering, fragility is represented by the probability of exceeding a certain damage measure (DM) given the occurrence of a particular intensity measure (IM):

$$P[d > DM \mid IM=x] \tag{2}$$

In this study, the probability has been mathematically expressed through a log-normal cumulative distribution function, as given by the following equation:

$$P[d > DM \mid IM=x]= 1- \Phi \left(\frac{\ln x - \ln \theta}{\beta}\right) \tag{3}$$

where $\Phi$ is the standard normal cumulative distribution function; $x$ is the variable of the intensity measure; $\theta$ is the median value of the intensity measure and $\beta$ is the standard deviation of the natural logarithm of the intensity measure.

In particular, the mean value was obtained from the linear regression analysis of the 70 data points obtained through the performed nonlinear time-history analyses using the equation stated below:

$$\theta =A+B\cdot \ln x \tag{4}$$

while the standard deviation of the natural logarithm was obtained as:

$$\beta =\sqrt{\textstyle\sum_{i=1}^{n} (d_i-\theta_i)^2 / (n-2)} \tag{5}$$

## 4.2 Limit states

For earth dams, different limit states relating to different collapse modes of the dam embankment may be identified. In this study, four damage measures (DMs) were considered to perform the IDA procedure and obtain the fragility curves (Table 3):

- Dimensionless settlement ratio in correspondence of the dam crest (DSR), i.e. the ratio of the vertical displacement of the dam crest to the total height of the dam body. According to the popular classification suggested by Swaisgood [15, 16, 17] or Pells and

Fell [18], three limit states were considered, i.e. 0.2% as minor damage, 0.5% as moderate damage and 1.0% as severe damage;
- the lateral displacements of the dam crest, with the damage thresholds proposed by Idriss [19], namely 15 cm as minor damage, 30 cm as moderate damage and 90 cm as severe damage;
- the freeboard reduction, i.e. the settlement of the upstream vertex of the crest divided by the initial freeboard. Damage thresholds equal to 25% as minor damage, 50% as moderate damage, and 65% as severe damage were considered;
- the maximum plastic shear strain of the watertightness element. This study refers to the classification proposed by Pang et al. [5], who considered three limit states equal to 1.5%, 2.5% and 3.5%, corresponding to minor, moderate and severe damage levels, respectively.

| **Damage measures** | **Threshold** | | |
|---|---|---|---|
| | **Minor** | **Moderate** | **Severe** |
| Settlement ratio (DSR) | 0.2% | 0.5% | 1.0% |
| Lateral displacement (LD) | 15 cm | 30 cm | 90 cm |
| Freeboard reduction (FR) | 25% | 50% | 65% |
| Plastic shear strain (PSS) | 1.5% | 2.5% | 3.5% |

Table 3: Threshold values of the three limit states considered for the damage measures of the small dam.

### 4.3 Results

Figures 5, 6 and 7 shows the fragility curves of the small zoned earth dam on rock foundation, obtained for three intensity measures (PGA, PGV and AI) and the four damage measures mentioned above.

As highlighted in the previous sections, the advantage of these curves is the possibility to obtain an expedited estimation of the possible damage suffered by the structure, once the intensity of the earthquake at the dam site has been estimated. This tool provides for an effective support to identify the critical response or weakness of the structure, which requires a prompt decision by the dam owner.

From all the fragility curves computed (Figures 5 - 7), it emerges that the damage mechanism likely to be mostly overcome is the dimensionless settlement ratio at the dam crest (DSR), followed by the plastic deformation of the watertightness element (PSS) for all the IMs considered (PGA, PGV and AI). Conversely, at first glance, the fragility curve corresponding to the freeboard reduction (FR) does not seem to be as representative as the others DMs. Such a noticeable difference between DSR and FR may be attributed to the damage thresholds that have been identified in literature for the FR measure, being these values not consistent with those assumed for DSR. This aspect has further been investigated in this study by regenerating the fragility curves corresponding to FR with lower thresholds than those listed in Table 3, that is 2% for minor, 6% for moderate and 10% for severe damage.

In Figure 8, the fragility curves of all DMs corresponding to minor and severe damage have been compared. This provides useful information on the probability of exceeding the serviceability or collapse state of the dam for a given value of the IM, provided for example by the seismic stations placed at the dam site.

Among the different intensity measures, it was observed that a lower standard deviation is associated to AI rather than PGA and PGV, as already highlighted in Sica et al. [20]. This supports the use of the Arias Intensity as primary IM for developing fragility curves of earth dams as it is widely ascertained that AI correlates better with the predicted damage of the dam embankment.

(a) (b) (c) (d)

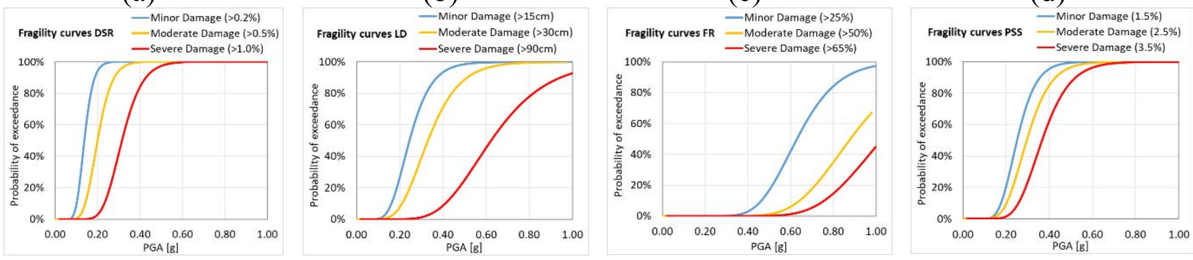


Figure 5: Fragility curves with PGA as intensity measure: (a) settlement ratio at the dam crest (DSR), (b) lateral displacement (LD), (c) freeboard reduction (FR) and (d) plastic shear strain of the watertightness element (PSS)

(a) (b) (c) (d)

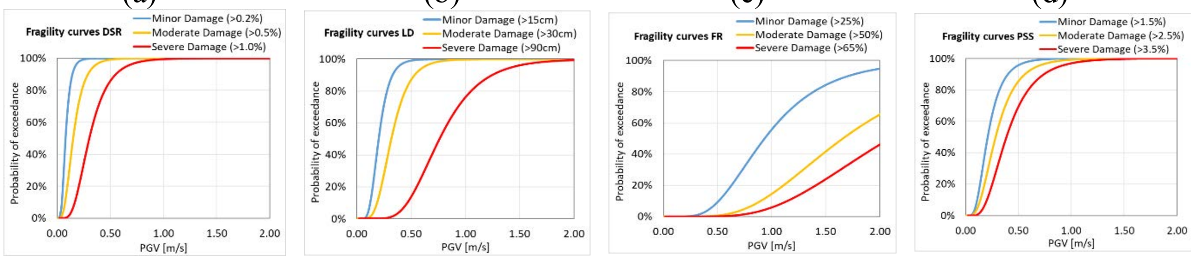


Figure 6: Fragility curves with PGV as intensity measure: (a) settlement ratio at the dam crest (DSR), (b) lateral displacement (LD), (c) freeboard reduction (FR) and (d) plastic shear strain of the watertightness element (PSS)

(a) (b) (c) (d)

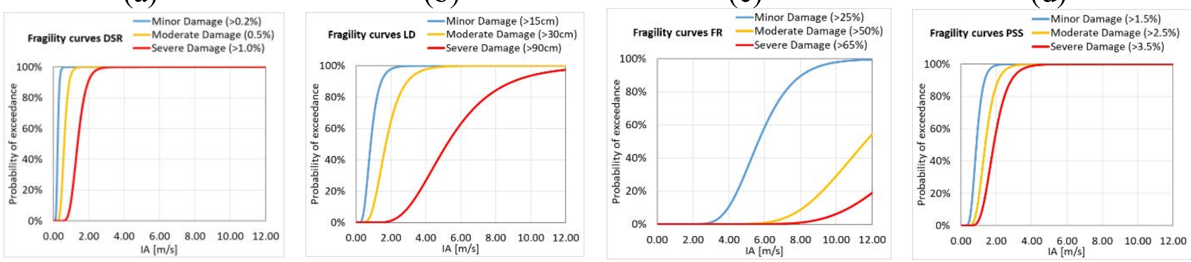


Figure 7: Fragility curves with AI as intensity measure: (a) settlement ratio at the dam crest (DSR), (b) lateral displacement (LD), (c) freeboard reduction (FR) and (d) plastic shear strain of the watertightness element (PSS)

(a) (b)

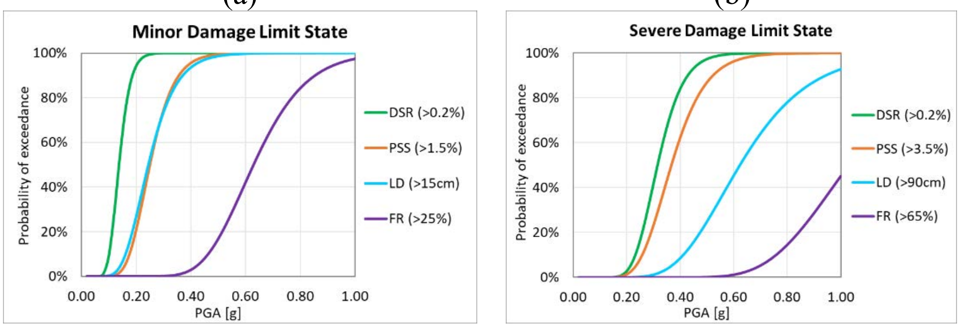


Figure 8: Comparison among the fragility curves for all the DMs considered in this study in case of minor (a) and severe (b) damage limit state.

As a further consideration, the probability of exceeding a certain damage level was evaluated for the limit states prescribed by the Italian technical code for dams [21, 22], assuming that the ideal small dam considered in this work is located on a rock outcrop in a zone characterized by medium-high seismic hazard. For a dam with a reference period $V_R$=75 years, the limit states imposed by the current Italian standards [21, 22] are listed in Table 4, with the corresponding probability of exceeding $P_{VR}$, return period $T_R$ and PGA.

| Limit state | $P_{VR}$ [%] | $T_R$ [years] | PGA [g] |
|---|---|---|---|
| OLS | 81 | 45 | 0.066 |
| DLS | 63 | 75 | 0.085 |
| VLS | 10 | 710 | 0.223 |
| CLS | 5 | 1460 | 0.282 |

Table 4: Limit states, return periods and maximum rock accelerations at the dam site.

Considering the dimensionless settlement ratio at the dam crest as the most sensitive damage measure, the probability of exceedance is almost null for all the damage levels corresponding to DLS. Conversely, for the CLS, there is the almost complete possibility of exceeding minor and moderate damage (100% and 85% respectively) and the 32% of probability of reaching the condition of severe damage. If the fragility curves provided in literature for large zoned earth dams are considered for comparison, it emerges a lower exceedance probability of the same limit states considered in this paper for the small dam on a rigid base. It is worth pointing out that the published fragility curves refer to large dams founded on deformable soil deposits. Therefore, as future perspective of the present study, fragility curves for small earth dams founded on non-rocky soils will be computed.

## 5 CONCLUSIONS

The paper proposed a suite of fragility curves to evaluate the seismic vulnerability of small earth dams. The selected case study is representative of a wider category of tailing or small earth dams, which are often disregarded in control activity, irrespectively of their generally high vulnerability. Fragility curves may be useful tools for a rapid post-earthquake damage assessment and also for planning future repair interventions. The obtained fragility curves indicate the probability that a certain damage level will be exceeded, given the occurrence of an intensity measure. To develop the fragility curves, the randomness of the input ground motion was taken into account and the seismic performance of the reference dam was assessed through finite element analyses considering four damage measures, i.e. the settlement ratio and the lateral displacements at the dam crest, the freeboard reduction and the maximum plastic shear strain of the watertightness element. As an outcome of the study, the Arias Intensity revealed to be the most sensitive intensity measure to assess dam damage. For the small dam considered in this study, among the different damage mechanisms considered, the settlement ratio at the dam crest and the plastic shear strain of the watertightness element presented the higher probability of being exceeded. As future perspective of this research study, additional parametric analyses accounting for the uncertainty related to soil properties and subsoil layer setting will be carried out.

## REFERENCES


[1] Alembagheri, M., & Ghaemian, M. Seismic assessment of concrete gravity dams using capacity estimation and damage indexes. *Earthquake Engineering & Structural Dynamics, 42*(1), 123-144, 2013.

[2] Alembagheri, M., & Ghaemian, M. Damage assessment of a concrete arch dam through nonlinear incremental dynamic analysis. *Soil Dynamics and Earthquake Engineering, 44*, 127-137, 2013.

[3] Hariri-Ardebili, M. A., & Saouma, V. E. Collapse fragility curves for concrete dams: comprehensive study. *Journal of Structural Engineering, 142*(10), 04016075, 2016.

[4] Bernier, C., Padgett, J. E., Proulx, J., & Paultre, P. Seismic fragility of concrete gravity dams with spatial variation of angle of friction: case study. *Journal of Structural Engineering, 142*(5), 05015002, 2016.

[5] Pang, R., Xu, B., Kong, X., & Zou, D. Seismic fragility for high CFRDs based on deformation and damage index through incremental dynamic analysis. *Soil Dynamics and Earthquake Engineering, 104*, 432-436, 2018.

[6] Pang, R., Xu, B., Zou, D., & Kong, X. Seismic performance assessment of high CFRDs based on fragility analysis. *Science China Technological Sciences, 62*, 635-648, 2019.

[7] Pang, R., Xu, B., Zhou, Y., Zhang, X., & Wang, X. Fragility analysis of high CFRDs subjected to mainshock-aftershock sequences based on plastic failure. *Engineering Structures, 206*, 110152, 2020.

[8] Jin, C., & Chi, S. Seismic fragility analysis of high earth-rockfill dams considering the number of ground motion records. *Mathematical Problems in Engineering, 2019*, 1-12, 2019.

[9] Ayati Ahmadi, A., Noorzad, A., MohammadNezhad, H., & Mirghasemi, A. A. Seismic Fragility of Rockfill Dams with Asphaltic Concrete Core. *Iranian Journal of Science and Technology, Transactions of Civil Engineering*, 1-14, 2022.

[10] Khalaj, O., Ayati Ahmadi, A., Abedin Nejad, S., Mašek, B., Štadler, C., & Skála, J. Evaluation of the effect of varying the angle of asphaltic concrete core on the behavior of the meijaran rockfill dam. *Coatings*, 12(6), 720, 2022.

[11] Boada, G., Pasten, C., & Heresi, P. Analytical fragility curves for abandoned tailings dams in North-Central Chile. *Soil Dynamics and Earthquake Engineering, 164*, 107637, 2023.

[12] Brinkgreve, R.B.J. PLAXIS 2D Manuals. General Information. Tutorial Manual. Reference Manual. Ma-terial Models Manual. Scientific Manual. Delft Univer-sity of Technology & PLAXIS. ISBN13.978(90). 76016, 2018.

[13] Hudson, M. A. R. T. I. N., Idriss, I. M., & Beikae, M. QUAD4M: a computer program to evaluate the seismic response of soil structures using finite element procedures and incorporating a compliant base. Center for Geotechnical Modeling, Department of Civil and Environmental Engineering, University of California, Davis, 1994.

[14] Hashash, Y. M., & Park, D. Viscous damping formulation and high frequency motion propagation in non-linear site response analysis. *Soil Dynamics and Earthquake Engineering, 22*(7), 611-624, 2002.

[15] Swaisgood, J. R. Embankment dam deformations caused by earthquakes. In *Pacific conference on earthquake engineering* (Vol. 14), 2003.

[16] Swaisgood J. R. Seismically-induced deformation of embankment dams. *In proceedings of sixth national conference on earthquake engineering. Seattle, Washington, U. S. A.*, 1998.

[17] Swaisgood, J. R., & Au-Yeung, Y. Behavior of dams during the 1990 Philippines earthquake. In *ASDSO Annual Conference*, 1991.

[18] Pells, S., & Fell, R. Damage and cracking of embankment dams by earthquakes and the implications for internal erosion and piping. University of New South Wales, School of Civil and Environmental Engineering, 2002.

[19] Idriss, I. M. Evaluating seismic risk in engineering practice. Proceedings of the eleventh international conference on soil mechanics and foundation engineering, San Francisco, 12-16. *Publication of: Balkema (AA)*, 1985.

[20] Sica, S. & Pagano, L. Performance-based analysis of earth dams: Procedures and application to a sample case. *Soils and Foundations* 49(6), pp. 921-939, 2009.

[21] MIT, Ministero delle Infrastrutture e dei Trasporti 2014. Norme tecniche per la progettazione e la costruzione degli sbarramenti di ritenuta (dighe e traverse). Decreto del Ministro 26 giugno 2014, Gazzetta Ufficiale n°156 del 08.07.2014 (in Italian), 2014.

[22] NTC2018, Norme tecniche per le costruzioni, D.M. 17/01/2018, Gazzetta Ufficiale n. 35 del 20.02.2018, Suppl. Ord. n.42, 2018. 2018.